mosaic spread evaluated [in *MADNES*; Messerschmidt & Pflugrath (1987)] as 3.4°. Both the large mosaic spread and the twinning may be associated with the variable Cu:Zn composition, and a simple explanation can be suggested: a region rich in zinc, with little or no copper, should have a structure like hydrozincite, *i.e.* with tetrahedral $M(3)$ on both sides of the oxygen double layer, whereas a copper content above a certain threshold presumably introduces distortions and leads to regions of aurichalcite structure with tetrahedral $M(3)$ and trigonal bipyramidal $M(4)$ on opposite sides of the double layer. The occasional insertion of the hydrozincite type of layer in the aurichalcite structure would lead to the observed twinning.

We are grateful to SERC for financial support and for the provision of synchrotron radiation facilities.

References

CERNIK, R. J. & BELL, A. (1994). *J. Appl. Cryst.* **27**. In preparation.

COUVES, J. W., THOMAS, J. M., WALLER, D., JONES, R. H., DENT, A. J., DERBYSHIRE, G. E. & GREAVES, G. N. (1992). *Nature*, **354**, 465–468.

CROMER, D. T. & LIEBERMAN, D. (1970). *J. Chem. Phys.* **53**, 1891–1898.

GHOSE, S. (1964). *Acta Cryst.* **17**, 1051–1057.

HELLIWELL, J. R., PAPIZ, M., GLOVER, I. D., HABASH, J., THOMPSON, A. W., MOORE, P. R., HARRIS, N., CROFT, D. & PANTOS, E. (1986). *Nucl. Instrum. Meth. Phys. Res. A*, **246**, 617–623.

JAMBOR, J. L. & POULIOT, G. (1965). *Can. Mineral.* **8**(3), 385–389.

JOYNER, R. W., KING, F., THOMAS, M. A. & ROBERTS, G. (1991). *Catal. Today*, **10**, 417–419.

MESSERSCHMIDT, A. & PFLUGRATH, J. W. (1987). *J. Appl. Cryst.* **20**, 306–315.

PAPIZ, M. Z. (1989). Personal communication.

POLLARD, A. M., SPENSER, M. S., THOMAS, R. G., WILLIAMS, P. A., HOLT, J. & JENNINGS, J. R. (1992). *Appl. Catal. A*, **86**, 1–11.

SHELDRICK, G. M. (1992). *SHELXL92. Program for the Refinement of Crystal Structures*. Univ. of Göttingen, Germany.

WALLER, D., STIRLING, D., STONE, F. S. & SPENCER, M. S. (1989). *Faraday Discuss. Chem. Soc.* **87**, 107–129.

Acta Cryst. (1994). B**50**, 676–684

Crystal Structure of the Commensurately Modulated ζ Phase of PAMC

BY P. HARRIS, F. K. LARSEN,* B. LEBECH AND N. ACHIWA†

Department of Solid State Physics, Risø National Laboratory, DK-4000 Roskilde, Denmark

(*Received* 31 *December* 1993; *accepted* 28 *March* 1994)

Abstract

The commensurately modulated ζ low-temperature phase of bis(propylammonium) tetrachloromanganate(II), $[NH_3(C_3H_7)]_2MnCl_4$, has been determined at 8 K. $a = 7.437\ (5)$, $b = 7.082\ (5)$, $c = 13.096\ (8)$ Å, $\alpha = 105.59\ (1)°$. Superspace group $P2_1/b(0\beta0)\bar{1}s$, with $\beta = 1/3$, $V = 664.4$, $Z = 2$, $D_x = 1.58$ g cm^{-3}, Mo $K\alpha$ radiation, $\lambda = 0.71069$ Å, $\mu = 17.99$ cm^{-1}, $F(000) = 326$, $wR(F) = 0.064$ for 1444 main reflections and $wR(F) = 0.089$ for 248 satellite reflections. The modulation vector flips and locks into a commensurate value compared with the ε phase, indicating a 'lock-in' and phase shift between adjacent modulated layers. The modulation waves do not change much from the values of the ε phase, which confirms the lock-in of the modulation vector; only some components of the modulations of the propylammonium chains appear to be significantly different, these chains appear to be responsible for the phase shift across the layers.

* Department of Chemistry, Århus University, DK-8000 Århus C, Denmark.

† Department of Physics, Kyushu University, Higashi-ku, Fukuoka, Japan.

1. Introduction

The layered perovskite PAMC, bis(propylammonium) tetrachloromanganate(II), belongs to a structural family of compounds of the general formula $(C_nH_{2n+1}NH_3)_2MX_4$, with $M = Mn^{2+}$, Cd^{2+}, Fe^{2+}, Cu^{2+}, Cr^{2+}, Pd^{2+} and $X = Cl^-$, Br^-. All these compounds consist of (MX_6) octahedra sandwiched between the alkylammonium chains (see Fig. 1 for a schematic structure). The compounds having $n = 3$ are unique as they exhibit the largest sequence of phase transitions (Depmeier, Felsche & Wildermuth, 1977; Depmeier, 1979). PAMC is additionally a two-dimensional antiferromagnet with a weak ferromagnetic moment and has been extensively studied both because of its structural and its magnetic properties.

The phase transitions are due to a gradual selection and ordering of the possible hydrogen bondings between the NH_3^+ groups and the Cl^- ions, followed by a reorientation of the propylammonium chains. The tendency of the methyl ends of the chains to form an energetically favourable hexagonally packed layer, along with the constraint imposed by a nearly quadratic arrangement of the Cl octahedra, creates a frustration leading to the introduction of several

© 1994 International Union of Crystallography
Printed in Great Britain – all rights reserved

different conformations (Chapuis & Doudin, 1991). The propylammonium chains of adjacent layers only interact through van der Waals' forces between the methyl groups and, therefore, PAMC has been called a crystalline model of lipid bilayers. The structural phase sequence with space group and phase transition temperature is as follows [see Depmeier (1986) for a review]: α phase $I4/mmm$; 441 K; β phase $Abma$; 388 K; γ phase $Abma(\alpha 01)s\bar{1}1$; 339 K; δ phase $Abma$; 168 K; ε phase $Abma(0\beta 0)s\bar{1}1$; 112 K; ζ phase $P2_1/b(0\beta 0)\bar{1}s$; 39 K; the magnetically ordered phase. In the high-temperature α phase the time-averaged symmetry of the structure is tetragonal, in the β–ε phases it is orthorhombic and in the low-temperature ζ phase no dynamical disorder persists, and the symmetry becomes monoclinic. The structures of the orthorhombic β–ε phases in the literature are described in an A-centred cell of approximate dimensions $a_o = 7.43$, $b_o = 7.10$, $c_o = 25.5$ Å. ζ-PAMC is monoclinic and the obvious unit-cell choice is the primitive cell $\mathbf{a}_m \approx \mathbf{a}_o$, $\mathbf{b}_m \approx \mathbf{b}_o$ and $\mathbf{c}_m \approx \frac{1}{2}(\mathbf{c}_o - \mathbf{b}_o)$, as suggested by Depmeier & Mason (1983).

The dynamical disorder of the propylammonium chains was observed by NQR–NMR spectroscopy (Muralt, Kind & Bührer, 1988) to persist down to 112 K. At 112 K the chains order and the crystal undergoes a phase transition from orthorhombic to monoclinic symmetry. At the same temperature, the modulation vector locks in from an incommensurate value of $(\frac{1}{3} + \delta)\mathbf{b}_o^*$ to a commensurate value of $\frac{1}{3}(\mathbf{b}_o^* + \mathbf{c}_o^*) = \frac{1}{3}\mathbf{b}_m^*$. The two directions are not parallel, thus the modulation vector turns at the lock-in transition – a very unusual behaviour. This paper is concerned with the structure of the low-temperature commensurately modulated ζ phase at 8 K.

2. Experimental

Crystals of PAMC were cut from a big crystal grown from an aqueous solution of $MnCl_2$ and $CH_3CH_2CH_2NH_3Cl$. The small crystals suffered from large mosaicity and gave weak reflections. Several crystals were tested at the diffractometer before we found one of reasonable quality. The chosen crystal was of the dimensions $0.4 \times 0.4 \times 0.1$ mm^3. It was fixed with silicon grease in a capillary, mounted in a type 202 Displex on an Huber four-circle diffractometer, located at Department of Inorganic Chemistry, University of Århus, Denmark. A graphite monochromator was used, selecting a wavelength of $\lambda = 0.71069$ Å from a molybdenum anode. The crystal was cooled to 8 K.

The lattice parameters were determined from centring 18 high-angle reflections, $30 < 2\theta < 47°$. The reflection pattern in the b^*c^*-plane is shown in Fig. 2; it is in agreement with observations by Depmeier & Mason (1983) and Achiwa, Matsuyama & Yoshinari (1990). Unlike the phases at temperatures above 112 K, the ζ phase shows multiple twinning in the bc-plane. The crystal is twinned in the sense that it contains two monoclinic domains with oppositely directed **c***-axes, as indicated in Fig. 2. Positive **a**- and **b**-axes of one twin individual are oriented along negative **a**′- and **b**′-axes of the other twin individual. As the **c**- and **c**′-axes are not parallel, the reflections split along the **c***-axis. The splitting was easily seen in a preliminary neutron experiment (Harris, Lebech

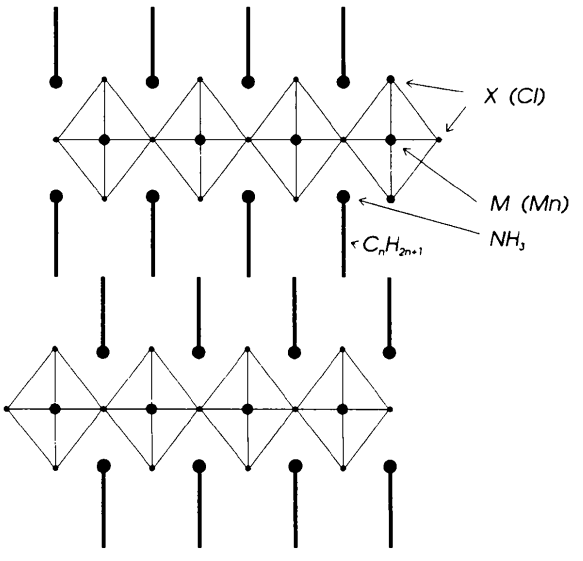

Fig. 1. A schematic structure of the $(C_nH_{2n+1}NH_3)_2MX_4$ compounds [see Blinc *et al.* (1977)].

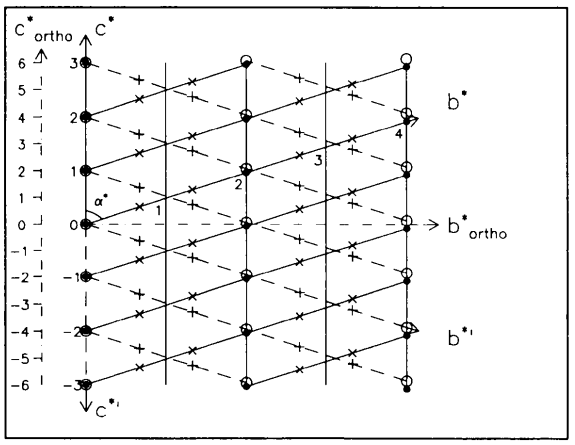

Fig. 2. The observed diffraction pattern in the bc-plane. • and × are the main and the relatively weak satellite reflections for one crystal orientation; ○ and + are the main and satellite reflections for the other crystal orientation. The unprimed and primed axes give the cells for the two crystal orientations, respectively. Due to the twinning, both cells are always present.

Table 1. *Fractional atomic positions, isotropic temperature factors and fractional modulation parameters*

	x	y	z	B_{iso} (Å)	U_x^{sin}	U_y^{sin}	U_z^{sin}	U_x^{cos}	U_y^{cos}	U_z^{cos}
Mn	0	0	0	1.99 (6)	−0.005 (1)	−0.004 (1)	−0.0127 (7)	0	0	0
Cl(1)	0.759 (1)	0.255 (1)	0.0192 (2)	2.03 (8)	−0.004 (2)	−0.000 (2)	0.001 (1)	−0.008 (2)	0.0077 (8)	0.0162 (6)
Cl(2)	0.0447 (3)	0.094 (2)	0.1939 (2)	2.6 (1)	−0.011 (2)	−0.010 (2)	−0.009 (1)	0.008 (2)	−0.028 (1)	0.003 (1)
N	−0.023 (1)	0.430 (4)	0.8305 (7)	1.9 (3)	−0.003 (4)	0.022 (4)	0.007 (4)	−0.015 (5)	−0.021 (4)	−0.006 (3)
C(1)	0.079 (1)	0.385 (4)	0.7274 (9)	2.3 (3)	−0.015 (5)	−0.035 (5)	−0.002 (4)	0.017 (6)	0.021 (6)	0.000 (4)
C(2)	−0.029 (2)	0.303 (4)	0.633 (1)	1.5 (4)	−0.051 (3)	0.061 (4)	−0.002 (2)	0.027 (4)	−0.035 (4)	0.002 (3)
C(3)	0.090 (2)	0.282 (5)	0.532 (1)	2.3 (4)	−0.049 (3)	−0.004 (5)	−0.006 (2)	0.014 (7)	−0.001 (5)	−0.004 (4)

Table 2. *Fractional atomic positions, isotropic temperature factors and fractional modulation parameters, where reflections having* $|F_o - F_c| > 10\sigma_o$ *have been omitted in the refinement*

	x	y	z	B_{iso} (Å)	U_x^{sin}	U_y^{sin}	U_z^{sin}	U_x^{cos}	U_y^{cos}	U_z^{cos}
Mn	0	0	0	1.76 (3)	−0.0052 (6)	−0.0058 (5)	−0.0125 (4)	0	0	0
Cl(1)	0.7562 (6)	0.2547 (7)	0.0191 (1)	1.94 (4)	−0.0067 (8)	−0.0025 (9)	0.0003 (6)	−0.001 (1)	0.0069 (4)	0.0153 (3)
Cl(2)	0.0458 (2)	0.0961 (9)	0.1940 (1)	2.15 (5)	−0.0109 (7)	−0.0108 (9)	−0.0100 (5)	−0.000 (1)	−0.0296 (5)	0.0012 (7)
N	−0.0228 (6)	0.427 (2)	0.8280 (4)	2.1 (1)	0.002 (2)	0.020 (2)	0.005 (2)	0.005 (3)	−0.023 (2)	−0.000 (2)
C(1)	0.0766 (8)	0.388 (2)	0.7280 (5)	1.9 (2)	−0.012 (3)	−0.031 (3)	−0.005 (2)	0.009 (3)	0.017 (3)	−0.006 (2)
C(2)	−0.017 (1)	0.303 (2)	0.6337 (7)	2.1 (1)	−0.055 (2)	0.072 (2)	0.000 (1)	0.010 (3)	−0.032 (2)	−0.004 (2)
C(3)	0.090 (1)	0.268 (4)	0.5322 (6)	2.6 (2)	−0.052 (2)	−0.009 (4)	−0.004 (1)	−0.004 (4)	−0.006 (2)	−0.002 (2)

& Achiwa, 1994), but because of the large crystal mosaicity it could not be resolved in this four-circle X-ray experiment.

Intensities of main reflections were collected in the pseudo-orthorhombic cell of dimensions 7.437 (5), 7.082 (5) and 25.22 (2) Å, which is similar to the unit cell for the orthorhombic phases of PAMC. The range in indices is $-7 \le h \le 7$, $0 \le k \le 6$, $-24 \le l \le 24$. 3535 data with $(\sin\theta/\lambda)_{max} = 0.53$ Å^{-1} were measured. Data collection for the satellite reflections was performed in an orthorhombic supercell of the dimensions 7.437 (5), 21.25 (1) and 75.65 (5) Å, with the range of indices $0 \le h \le 4$, $-5 \le k \le 13$, $-14 \le l \le 28$. A total of 665 satellite intensities with $(\sin\theta/\lambda)_{max} = 0.53$ Å^{-1} were measured. The temperature varied between 7.9 and 8.1 K during the data collection. An ω–2θ step scan procedure was used with 75 steps in a scan of width $\Delta\theta$ at values of θ as follows; $\Delta\theta,\theta = 0.80,0$; 0.90,15; 1.10,30; 1.50,45; 2.10,60°. Counting time per step was 2 s for main reflections and 20 s for the relatively weak satellite reflections.

Lorentz and polarization corrections and a Gaussian absorption correction with 432 sampling points were applied (Coppens, Leiserowitz & Rabinowich, 1965). Maximum and minimum transmission was 0.83 and 0.51. After removing the systematically extinct reflections of the pseudo-orthorhombic cell, hkl, $k + l = 2n + 1$, data were sorted and averaged to give 1991, of which 1843 had positive intensity. The agreement between equivalent reflections is $R_I = 0.069$.

The lattice parameters were converted to the monoclinic cell

$$\mathbf{a}_m = \mathbf{a}_o; \qquad a = 7.437\ (5);$$
$$\mathbf{b}_m = \mathbf{b}_o; \qquad b = 7.082\ (5);$$
$$\mathbf{c}_m = \tfrac{1}{2}(\mathbf{c}_o - \mathbf{b}_o); \qquad c = 13.096\ (8)\ \text{Å}.$$

As we were not able to measure the monoclinic splitting, our *measured* value of α was

$$\alpha = 90° + \tan^{-1}\frac{b_o}{c_o} = 105.69\ (1)°.$$

However, b_o and c_o are not longer perpendicular in the ζ phase (Depmeier, 1986) and the correct value is

$$\alpha = 90° + \tan^{-1}\frac{b_o}{c_o} = 0.176\ (3)° = 105.51°,$$

where 0.176° is the change in monoclinic angle determined at 8 K by a single-crystal neutron scattering experiment (Harris, Lebech & Achiwa, 1994).

The Miller indices were converted accordingly: $h = h_o$; $k = k_o$; $l = \frac{1}{2}(l_o - k_o)$. Each reflection is given four indices, ($hklm$) so that the main reflections are indexed ($hkl0$) and satellite reflections ($hklm$). A reflection ($h,k,l,\pm 1$) is at the position ($h,k \pm \frac{1}{3},l$) when using conventional Miller indices. Reflections with integers k and l were main reflections with $m = 0$, reflections with Miller index $k + \frac{1}{3}$ had $m = 1$, reflections with Miller index $k - \frac{1}{3}$ had $m = -1$. Satellite reflections with non-integer l had their indices converted into the system of the twinned component.

The ($hkl0$) reflection from one twin individual is superimposed by the ($\bar{h},k,\bar{k} + \bar{l},0$) reflection from the other twin individual. The modulation vector is $\frac{1}{3}\mathbf{b}^*$. Fig. 2 shows that the satellite reflections from the two twin components appear at separate positions in reciprocal space.

3. Structure determination

A modulated stucture can be described in a superspace group, which can be determined from systematic absences of reflection intensity (de Wolff, Janssen & Janner, 1981). From observation of the reflections, the following reflection conditions were derived:

$0klm$; $k + m = 2n$, $h000$; $h = 2n$, corresponding to the superspace group $P2_1/b(0\beta0)\bar{1}s$ with $\beta = \frac{1}{3}$. The superspace group $P2_1/b(0\beta0)\bar{1}s$ is not given by de Wolff *et al.* (1981), but if we change the modulation vector to be $\frac{2}{3}\mathbf{b}^*$ ($\beta = \frac{2}{3}$, outside the first Brillouin zone), the reflection conditions would be $0klm$, $k = 2n$ and $h000$; $h = 2n$, leading to superspace group $P2_1/b(0\beta0)\bar{1}1$, which is number 14*a* listed by de Wolff, Janssen & Janner (1981). The two choices (1) $P2_1/b(0\beta0)\bar{1}s$, with $\beta = \frac{1}{3}$ and the fourfold general positions $\pm(x, y, z, t)$, $\pm(\bar{x} + \frac{1}{2}, y + \frac{1}{2}, z, t + \frac{1}{2})$, and (2) $P2_1/b(0\beta0)\bar{1}1$, with $\beta = \frac{2}{3}$ and the fourfold general positions $\pm(x, y, z, t)$, $\pm(\bar{x} + \frac{1}{2}, y + \frac{1}{2}, z, t)$, are equivalent (see Yamamoto, Janssen, Janner & de Wolff, 1985). Because the space group $P2_1/b$ can be transformed to $P2_1/n$, our result is also consistent with the result of Muralt, Kind & Bührer (1988), who from NMR spectroscopy determined the superspace group to be $P2_1/n(0\beta0)\bar{1}1$.

We could also have chosen to describe the structure in a big non-modulated unit cell **a**, 3**b**, **c**. The systematic extinctions would then be $0kl$; $k = 2n + 1$ and $h00$; $h = 2n + 1$ and the conventional space group $P2_1/b$. There are, however, two reasons for choosing the modulated description; first, all the satellite reflections are very weak compared with the main reflections, and a refinement in the big cell would be difficult to perform, second, when comparing with the ε phase, the commensurately modulated structure is the obvious choice. The apparent reduction in the degrees of freedom when using the modulation wave approach is the consequence of ignoring symmetry-allowed second harmonic modulation waves – this is reasonable because the observed first-order satellite reflections are of weak intensity (see Pérez-Mato, 1991). Refinements were performed with the program *JANA*93 (Petříček, Coppens & Becker, 1985; Petříček & Coppens, 1988) for both the average and the modulated structure. We decided to use only reflections with a positive observed intensity in the refinement, leaving 1590 main reflections and 253 satellite reflections.

The average structure was refined in space group $P2_1/b$ with the starting parameters taken from the δ phase (Depmeier & Mason, 1978). Only the Mn atom was on a special position and no split-atom model had to be used, as all dynamical disorder is frozen out at 8 K. The twinning was incorporated in the model. The *R*-factors reduced to $R = 0.115$ and $wR = 0.115$ for 1590 main reflections and 27 variables.

The modulated structure was refined in space group $P2_1/b(0\beta0)\bar{1}s$ (*JANA*93 has a commensurate option). We chose $\tau_4 = 0$ to generate an inversion centre at the origin, $\{I/0000\}$. The Mn atoms were then modulated with a sine wave only (being at a special position) and all other atoms were modulated with a sine and a cosine wave, so that their deviation from the average position was described as

$$\mathbf{U}_i = \mathbf{U}_i^{\sin} \sin(2\pi\mathbf{q}\cdot\mathbf{r}_i) + \mathbf{U}_i^{\cos} \cos(2\pi\mathbf{q}\cdot\mathbf{r}_i) \quad \mathbf{q} = \tfrac{1}{3}\mathbf{b}^* \quad (1)$$

All atoms were refined with isotropic thermal parameters. Weights of $\sigma^{-2}(F)$ were applied. All reflections with positive F_o were used as observed reflections, otherwise too many reflections would have been omitted.

The twinning was incorporated in the refinement. *JANA*93 makes it possible to use the common main reflections for twin individuals and also both sets of non-superimposed satellites (van Smaalen &

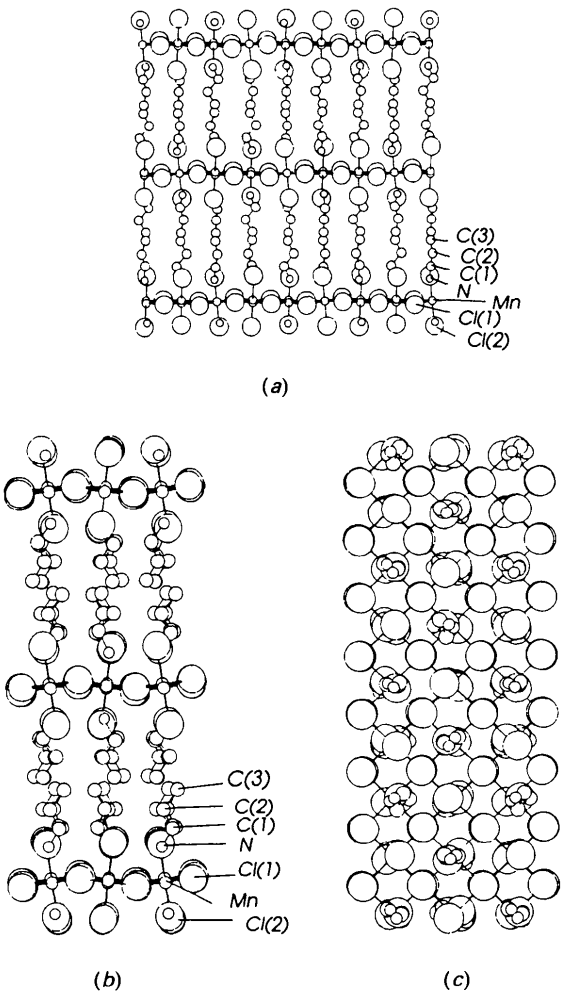

Fig. 3. The superstructure of ζ-PAMC. The atoms are shown with a radius proportional to their atomic [N, C(1), C(2), C(3)] or ionic [Mn, Cl(1), Cl(2)] radius. In (*a*) the **b** axis is horizontal and the **c*** axis is vertical. The modulation of the propylammonium chains along **b** may be noted. In (*b*) the structure is turned 90° around **c*** and is shown with **a** horizontal and **b** perpendicular to the plane of the paper. The modulations perpendicular to **b** are seen to be along **a** for the propylammonium chains and along **c*** for the $MnCl_6$ octahedra. (*c*) is a view down **c***.

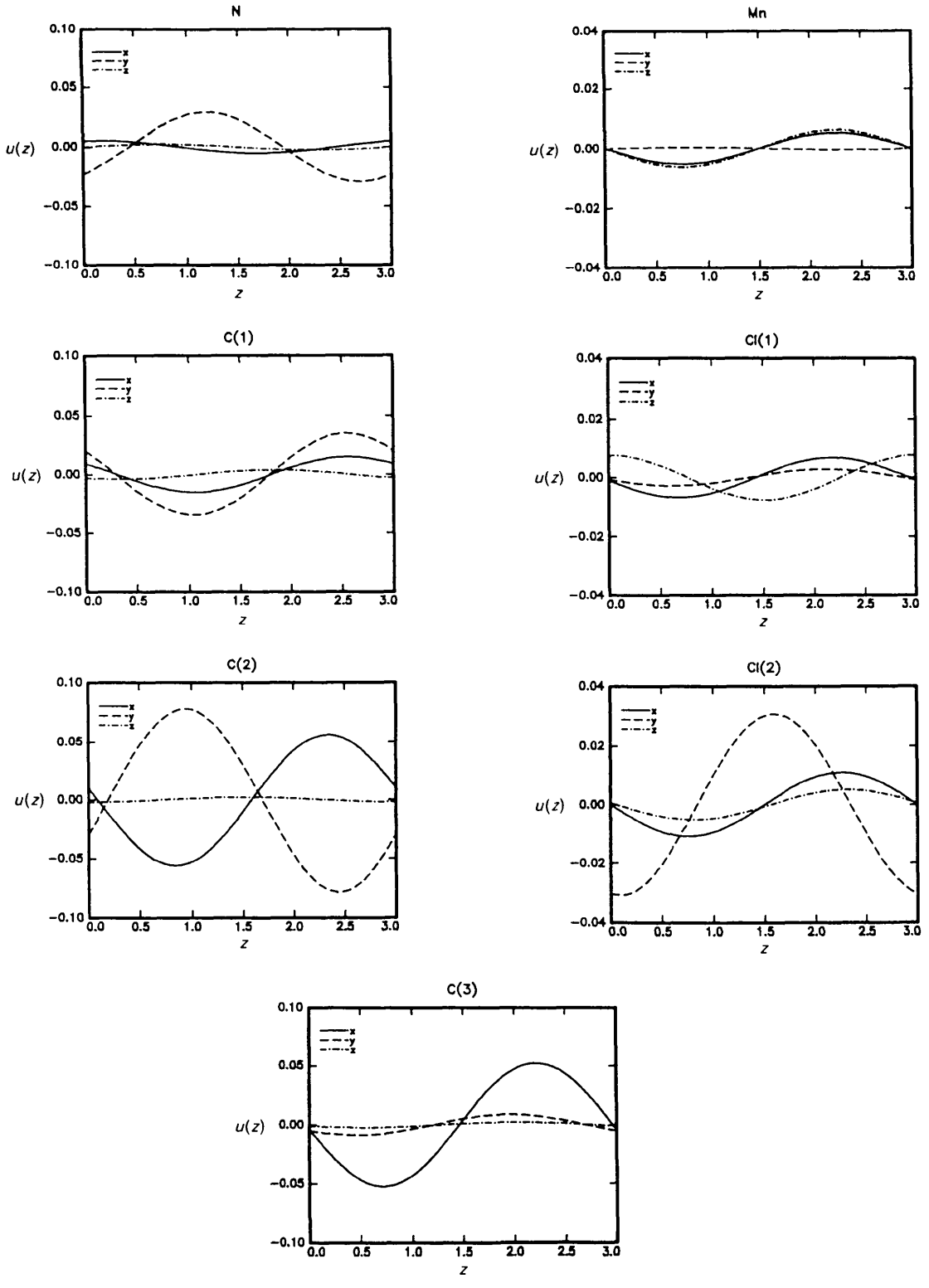

Fig. 4. The atomic modulations in the ζ and ε phases as a function of $z = 3t_4$, where t_4 is the so-called internal modulation parameter. (*a*) The values of the ζ phase in Table 2, converted to the pseudo-orthorhombic cell.

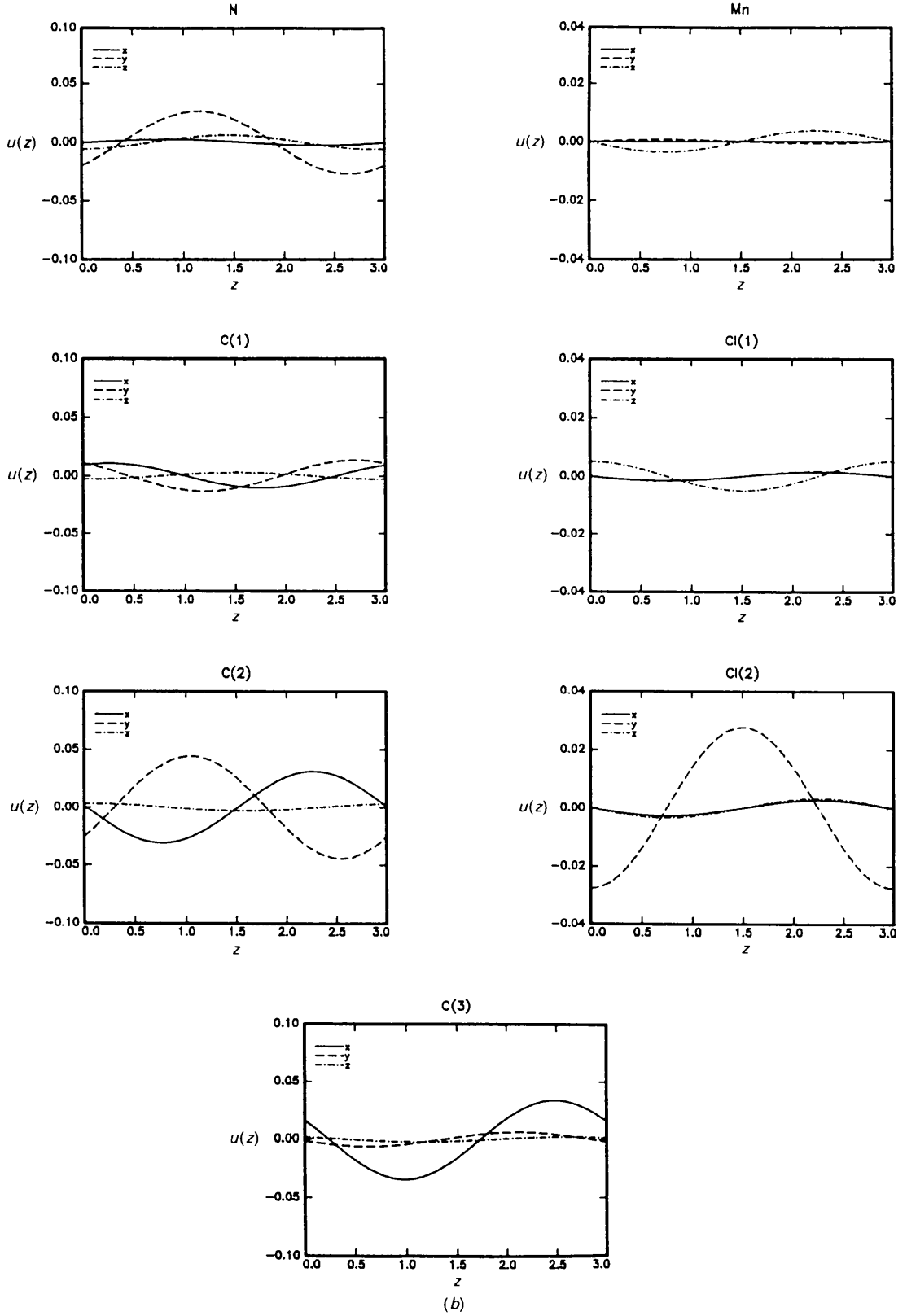

(*b*)

Fig. 4. (*b*) The values of the ε phase of Steurer & Depmeier (1989), using the commensurate approximation of $z = 3t_4$.

Petříček, 1992). Such a description can be obtained in several ways. We gave satellites ($m = \pm 1$) from the first twin component indices ($h,k,l,\pm 3$) and satellites from the second twin component indices ($h,k,l,\pm 2$). The indices of all reflections were divided by (1,1,1,3) so that the values read by the programme were ($h,k,l,\pm 1$) and ($h,k,l,\pm 2/3$), respectively. The twinning matrix (converting the indices from the first to the second twin component) was set to

$$\begin{pmatrix} -1 & 0 & 0 & 0 \\ 0 & 1 & 0 & 0 \\ 0 & -1 & -1 & 0 \\ 0 & 0 & 0 & 1.5 \end{pmatrix}.$$

This means that initially, satellites originating from the second twin component have the non-integer m and thus are not included in the structure-factor calculations from the first twin component. When the contribution from the second twin component is considered, the satellites belonging to the first twin component are transformed by the twinning matrix to ($h',k',l',\pm 1.5$) and satellites belonging to the second twin component are transformed to ($h',k',l',\pm 1$); in this case, satellites from the first twin component have the non-integer m and thus are not included in the structure-factor calculation.

The final R-factors were $R = 0.113$, $wR = 0.113$ [$R_{obs} = 0.097$, $wR_{obs} = 0.112$ for reflections with $I > 2.5\sigma(I)$] with $S = 6.4$ for all 1843 reflections and 66 variables. Partial R-factors were: $R = 0.107$, $wR = 0.112$ ($R_{obs} = 0.095$, $wR_{obs} = 0.112$) for 1590 main reflections and $R = 0.274$, $wR = 0.130$ ($R_{obs} = 0.179$, $wR_{obs} = 0.122$) for 253 satellite reflections. The parameters for this refinement are given in Table 1.*

To reduce the large values of S and the R-factors, we tried to include H atoms at ideal positions. This did not reduce the values significantly; probably a twinning effect in agreement with the fact that we were only able to measure reflections of significant intensity up to $2\theta = 45°$. We tried to remove from the refinement reflections with $|F_o - F_c| > 10\sigma_o$. This left us with 1444 main reflections and 248 satellite reflections. The R-factors reduced to $R = 0.086$, $wR = 0.066$ ($R_{obs} = 0.071$, $wR_{obs} = 0.065$) with $S = 3.3$ for all 1652 reflections and 66 variables. Partial R-factors were: $R = 0.082$, $wR = 0.064$ ($R_{obs} = 0.069$, $wR_{obs} = 0.063$) for 1444 main reflections and $R = 0.190$, $wR = 0.089$ ($R_{obs} = 0.127$, $wR_{obs} = 0.086$) for 248 satellite reflections. The parameters from this refinement are given in Table 2. The main difference between the parameters in Tables 1 and 2 is the thermal parameters. It is notable that even though only five satellite reflections were observed as bad reflections, the R-factor for the satellites is reduced by 30%. Main reflections with large deviations were all series of fixed h and k with l varying over a range of values. Otherwise, there were no obvious connections between them; they were measured continuously throughout the experiment and they were not lying at any particular positions in reciprocal space.

* A list of structure factors has been deposited with the IUCr (Reference: AB0321). Copies may be obtained through The Managing Editor, International Union of Crystallography, 5 Abbey Square, Chester CH1 2HU, England.

4. Discussion

Fig. 3 shows views of the superstructure from different directions. Fig. 3(*a*) has the **b** axis horizontal and it is easy to see the longitudinal modulation of the propylammonium chains. Fig. 3(*b*) has the **b** axis pointing into the plane of the paper and it shows that the transverse modulations of the propylammonium chains mainly are in-plane (along **a**), while the transverse modulations of the $MnCl_6$ octahedra are a combination of both in-plane and out-of-plane movements. Fig. 3(*c*) is a top view of the structure.

The values of the modulation functions in Table 2 have been converted into the pseudo-orthorhombic cell and inserted in (1). In Fig. 4(*a*) the resulting $\mathbf{U}_i$ are plotted as a function of $z = 2\pi(\mathbf{q}\cdot\mathbf{r}_i)$, to give a more quantitative impression of the modulation functions. It should be noted here, that only a finite set of points are relevant at these curves, as the structure is commensurately modulated. This is the set of points where $\mathbf{r}_i$ is an atomic position. In Fig. 4(*b*) we have plotted the atomic modulations for the ε phase (Steurer & Depmeier, 1989), assuming that this phase has a commensurate modulation of $\frac{1}{3}\mathbf{b}_o^*$. Comparison of the modulation waves for the ε and ζ phases does not yield large differences in the movement of the individual atoms and indeed, the ζ phase looks like a lock-in of the ε phase. The refinement of the modulation of the ζ phase was started from scratch and the result has, therefore, not been forced to similarity with the ε phase. Some differences are, however, apparent.

(1) The modulation amplitudes along the x direction of Mn, Cl(1) and Cl(2) are significantly larger in the ζ phase compared with the ε phase (the standard deviation for those three are all about 0.001). The modulation amplitudes along the y direction are almost unchanged. That is, the in-plane transverse wave has become more pronounced for these atoms.

(2) The modulations of N and C(3) are almost unchanged by the phase transition.

(3) C(1) has a larger modulation amplitude along the y-direction in the ζ phase compared with the ε phase (the standard deviation is within 0.003). The in-plane longitudinal modulation is more pronounced.

(4) C(2) has larger modulation amplitudes along both the x- and y-directions in the ζ phase compared with the ε phase (the standard deviations are all within 0.003). That is, the in-plane transverse and longitudinal modulations become more pronounced.

The symmetry operations of superspace group $P2_1/b(0\beta0)\bar{1}s$ are

$$(0,0,0,0)+$$
$$\pm(x,y,z,t), \quad \pm(\bar{x}+\tfrac{1}{2},y+\tfrac{1}{2},z,t+\tfrac{1}{2}), \qquad (2)$$

and the symmetry operations of the A-centred superspace group of the ε phase $Abma(0\beta0)s\bar{1}1$ (solved by Steurer & Depmeier, 1989) are

$$(0,0,0,0)+ \qquad (0,\tfrac{1}{2},\tfrac{1}{2},0)+$$
$$\pm(x,y,z,t), \quad \pm(\bar{x}+\tfrac{1}{2},y+\tfrac{1}{2},z,t+\tfrac{1}{2})$$
$$\pm(x,\bar{y},z,t), \quad \pm(\bar{x}+\tfrac{1}{2},\bar{y}+\tfrac{1}{2},z,t+\tfrac{1}{2}). \qquad (3)$$

Since the relation between the monoclinic and the orthorhombic unit-cell description is $\mathbf{a}_m = \mathbf{a}_o$, $\mathbf{b}_m = \mathbf{b}_o$ and $\mathbf{c}_m = \frac{1}{2}(\mathbf{c}_o - \mathbf{b}_o)$, the A-centring of the main structure of the orthorhombic ε phase is equivalent to a translation $\mathbf{c}_m + \mathbf{b}_m$ in the monoclinc ζ phase. The m_y mirror plane in the ε phase is due to the dynamical disorder of the crystal, as the propylammonium chains flip across the mirror plane. The general positions in the two space groups are, therefore, the same, the modulation functions in the two crystalline phases are very similar and as a whole one may conclude that the relative orientations of molecules and atoms in-plane are not affected at the transition. Fig. 5 is an attempt to illustrate the phase relation $[2\pi(\mathbf{q}\cdot\mathbf{r}_i + \tau)]$ between different lattice sites in the bc-plane for the ε and ζ structures, respectively, following the superspace group symmetries in (2) and (3) and the two different values of the $\mathbf{q}$ vectors. It is apparent that the only effect the crystalline phase transition has on the structure, except for the lock-in, is a phase shift across adjacent layers. The strongest interactions across the layers are sterical hindering and van der Waals' forces between adjacent CH_3 groups. These latter forces actually hold the crystal together. Changes in the interactions between CH_3 groups when ordering must be responsible for the turning of the modulation vector. When disordered (ε), the CH_3 groups take up more physical space and the sterical hindering must change at the transition. Also, when the crystal is in its disordered phase, there are different interaction constants from one CH_3 group to each of the two mirror images of the CH_3 group in the layer above. In the ordered phase (ζ), there has to be only one interaction constant and the orientation with the lowest energy does not necessarily have to be one of the two orientations present in the ε phase. The whole propylammonium chain will be affected and it is, therefore, not surprising that the most pronounced difference in the modulated structure lies in the propylammonium chain in C(1) and C(2). It is a bit surprising, though, that the movements of N and C(3) do not seem to be much affected at the phase transition.

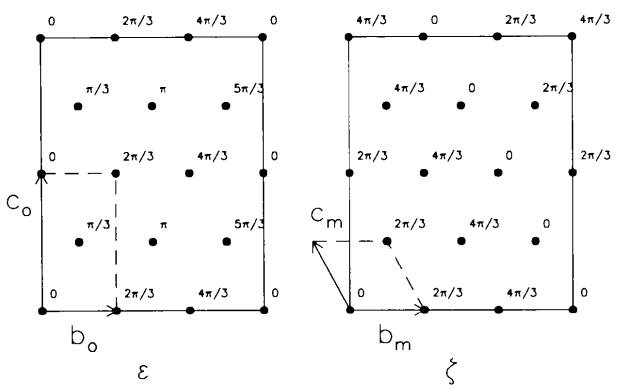

Fig. 5. The relative phases for different lattice points in the bc-plane for PAMC. (a) Relative phases in the ε phase (using commensurate approximation) for space group $P^{Abma}_{s\bar{1}1}$; (b): relative phases in the ζ phase for space group $P^{P2_1/b}_{\bar{1}'s}$.

The crystalline phase transition between the ε and the ζ phases is triggered by the ordering of the hydrogen bonds between the propylammonium chains and the Cl^- ions. This forces the crystal structure to become monoclinic, but does not automatically imply a lock-in and a rotation of the modulation vector. The fact that the three occur simultaneously indicates strong correlations between them. We hope that our result will, together with all the previous work done on PAMC, help to shed light on the mechanisms driving the phase transition at 112 K.

To investigate the system further, we have performed a neutron scattering experiment where the monoclinic distortion and the satellite intensities have been followed as a function of temperature. This work will be published elsewhere (Harris, Lebech & Achiwa, 1994).

Anette Frost Jensen from Department of Chemistry, Århus University, Denmark, and Václav Petříček from Institute of Physics, Academy of Science, Czech Republic, are acknowledged for help and fruitful discussions. We are indepted to the Carlsberg Foundation for diffractometer and cooling equipment.

References

ACHIWA, N., MATSUYAMA, T. & YOSHINARI, T. (1990). *Phase Transit.* **28**, 79–97.

BLINC, R., BURGAR, M., LOŽAR, B., SELIGER, J., SLAK, J., RUTAR, V., AREND, H. & KIND, R. (1977). *J. Chem. Phys.* **66**, 278–287.

CHAPUIS, G. & DOUDIN, B. (1991). In *Methods of Structural Analysis of Modulated Structures and Quasicrystals*, pp. 391–396. Singapore: World Scientific.
COPPENS, P., LEISEROWITZ, L. & RABINOWICH, D. (1965). *Acta Cryst.* **18**, 1035–1038.
DEPMEIER, W. (1979). *J. Solid. State Chem.* **29**, 15–26.
DEPMEIER, W. (1986). *Ferroelectrics*, **66**, 109–123.
DEPMEIER, W., FELSCHE, J. & WILDERMUTH, G. (1977). *J. Solid State Chem.* **21**, 57–65.
DEPMEIER, W. & MASON, S. A. (1978). *Acta Cryst.* B**34**, 920–922.
DEPMEIER, W. & MASON, S. A. (1983). *Solid State Commun.* **46**, 409–412.
HARRIS, P., LEBECH, B. & ACHIWA, B. (1994). *J. Phys. Condens. Matter*, **6**, 3899–3907.
MURALT, P., KIND, R. & BÜHRER, W. (1988). *Phys. Rev. B*, **38**, 666–679.
PÉREZ-MATO, J. M. (1991). In *Methods of Structural Analysis of Modulated Structures and Quasicrystals*, pp. 117–128. Singapore: World Scientific.
PETŘÍČEK, V. & COPPENS, P. (1988). *Acta Cryst.* A**44**, 235–239.
PETŘÍČEK, V., COPPENS, P. & BECKER, P. (1985). *Acta Cryst.* A**41**, 478–483.
SMAALEN, S. VAN & PETŘÍČEK, V. (1992). *Acta Cryst.* A**48**, 610–618.
STEURER, W. & DEPMEIER, W. (1989). *Acta Cryst.* B**45**, 555–562.
WOLFF, P. M. DE, JANSSEN, T. & JANNER, A. (1981). *Acta Cryst.* A**37**, 625–636.
YAMAMOTO, A., JANSSEN, T., JANNER, A. & DE WOLFF, P. M. (1985). *Acta Cryst.* A**41**, 538–530.

Acta Cryst. (1994). B**50**, 684–694

Intermolecular Interactions of Sulfonated Azo Dyes: Crystal Structures of the Diammonium, Dilithium, Magnesium and Calcium Salts of 7-Hydroxy-8-(phenylazo)-1,3-naphthalenedisulfonic Acid (Orange G)

WILLIAM H. OJALA, LINH KHANH LU, KEVIN E. ALBERS AND WILLIAM B. GLEASON

Department of Laboratory Medicine and Pathology and the Biomedical Engineering Center, University of Minnesota, Minneapolis, MN 55455, *USA*

TIMOTHY I. RICHARDSON AND REX E. LOVRIEN

Department of Biochemistry, University of Minnesota, St Paul, MN 55108, *USA*

AND ELISE A. SUDBECK

Department of Chemistry, University of Minnesota, Minneapolis, MN 55455, *USA*

(*Received* 3 *December* 1993; *accepted* 16 *May* 1994)

Abstract

The crystal structures of four salts containing the Orange G dianion have been determined, three at low temperature. Diammonium Orange G, $C_{16}H_{10}N_2O_7S_2(NH_4)_2.4H_2O$, forms triclinic crystals, space group $P\bar{1}$ (No. 2), with $a = 9.165$ (1), $b = 10.149$ (4), $c = 12.623$ (1) Å, $\alpha = 87.43$ (2), $\beta = 88.07$ (1), $\gamma = 71.00$ (2)°, $V = 1108.8$ (8) Å^3, $Z = 2$, $T = 173$ K, Cu $K\alpha$, $\lambda = 1.54178$ Å, $M_r = 514.52$, $D_x = 1.541$ g cm^{-3}, $\mu = 27.24$ cm^{-1}, $F(000) = 540$, $R = 0.048$ for 3471 observed reflections. Dilithium Orange G, $C_{16}H_{10}N_2O_7S_2Li_2.8H_2O$, forms triclinic crystals, space group $P\bar{1}$ (No. 2), with $a = 9.589$ (1), $b = 10.495$ (1), $c = 14.208$ (2) Å, $\alpha = 99.61$ (1), $\beta = 100.58$ (1), $\gamma = 115.81$ (1)°, $V = 1215.2$ (8) Å^3, $Z = 2$, $T = 173$ K, Cu $K\alpha$, $\lambda = 1.54178$ Å, $M_r = 564.39$, $D_x = 1.542$ g cm^{-3}, $\mu = 26.25$ cm^{-1}, $F(000) = 588$, $R = 0.030$ for 3862 observed reflections. Magnesium Orange G, $C_{16}H_{10}N_2O_7S_2Mg.8H_2O$, forms triclinic crystals, space group $P\bar{1}$ (No. 2), with $a = 8.844$ (1), $b = 10.179$ (1), $c = 13.901$ (1) Å, $\alpha = 79.18$ (1), $\beta = 79.49$ (1), $\gamma = 79.49$ (1)°, $V = 1194.2$ (5) Å^3, $Z = 2$, $T = 173$ K, Cu $K\alpha$, $\lambda = 1.54178$ Å, $M_r = 574.81$, $D_x = 1.598$ g cm^{-3}, $\mu = 29.46$ cm^{-1}, $F(000) = 600$, $R = 0.041$ for 4148 observed reflections. Calcium Orange G, $C_{16}H_{10}N_2O_7S_2Ca.9H_2O$, forms monoclinic crystals, space group $P2_1/n$ (No. 14), with $a = 9.395$ (4), $b = 27.492$ (9), $c = 10.368$ (2) Å, $\beta = 111.62$ (3)°, $V = 2489$ (3) Å^3, $Z = 4$, $T = 297$ K, Mo $K\alpha$, $\lambda = 0.71073$ Å, $M_r = 608.60$, $D_x = 1.624$ g cm^{-3}, $\mu = 4.82$ cm^{-1}, $F(000) = 1272$, $R = 0.039$ for 3083 observed reflections. Molecular geometry and conformation of the dye molecule are closely similar from structure to structure. In each case, the molecule exists as the hydrazo tautomer rather than as the azo tautomer. A recurring close intermolecular contact is a bridging interaction in which two water

©1994 International Union of Crystallography
Printed in Great Britain – all rights reserved